

ORIGINAL ARTICLE

Mid-infrared dual-comb spectroscopy with electro-optic modulators

Ming Yan^{1,2}, Pei-Ling Luo^{1,2}, Kana Iwakuni^{1,2}, Guy Millot³, Theodor W Hänsch^{1,2} and Nathalie Picqué^{1,2,4}

Absorption spectroscopy of fundamental ro-vibrational transitions in the mid-infrared region provides a powerful tool for studying the structure and dynamics of molecules in the gas phase and for sensitive and quantitative gas sensing. Laser frequency combs permit novel approaches to perform broadband molecular spectroscopy. Multiplex dual-comb spectroscopy without moving parts can achieve particularly high speed, sensitivity and resolution. However, achieving Doppler-limited resolution in the mid-infrared still requires overcoming instrumental challenges. Here we demonstrate a new approach based on difference-frequency generation of frequency-agile near-infrared frequency combs that are produced using electro-optic modulators. The combs have a remarkably flat intensity distribution, and their positions and line spacings can be freely selected by simply dialing a knob. Using the proposed technique, we record, in the 3- μm region, Doppler-limited absorption spectra with resolved comb lines within milliseconds, and precise molecular line parameters are retrieved. Our technique holds promise for fast and sensitive time-resolved studies of, for example, trace gases.

Light: Science & Applications (2017) 6, e17076; doi:10.1038/lsa.2017.76; published online 20 October 2017

Keywords: Fourier transform spectroscopy; frequency comb; mid-infrared; molecular spectroscopy

INTRODUCTION

Laser frequency combs¹ and their broad spectrum of evenly spaced narrow lines with precisely known positions provide novel opportunities for broadband molecular spectroscopy. In the last decade, a number of promising new techniques and experimental schemes interrogating the sample with a frequency comb have been demonstrated and perfected^{2–9}. Among such techniques, dual-comb spectroscopy, which measures the time-domain interference between two combs of slightly different line spacings, has the distinguishing advantage of providing a multiplex instrument without moving parts. Similar to a Michelson-based Fourier transform spectrometer, all the spectral elements are simultaneously measured on a single photodetector. Unlike the Michelson interferometer, however, the phase difference is automatically scanned with a static device. This feature potentially enables fast measurement speeds and high resolution in virtually any spectral region from the THz range to the extreme ultraviolet, as well as self-calibration of the frequency scale up to the accuracy of an atomic clock. Dual-comb spectroscopy also presents specific instrumental challenges that must be overcome before the technique can reach its full potential. The mid-infrared spectral range, where most molecules in the gas phase have strong fundamental ro-vibrational transitions, is extremely useful for precise high-resolution laboratory spectroscopy and for applications to, for example, trace gas detection. Mid-infrared laser frequency comb generation is still a technology under active development^{10–15}. Many

promising proof-of-principle experiments of dual-comb spectroscopy have been demonstrated with a variety of frequency comb sources, including quantum cascade lasers directly emitting in the mid-infrared^{16,17}, solid-state lasers emitting at the edge of the mid-infrared region¹⁸, synchronously pumped optical parametric oscillators^{19–21}, laser systems based on difference-frequency generation^{2,3,22,23} and micro-resonators²⁴. However, spectra at Doppler-limited resolution have only been reported once²², around 3 μm , with fully optically stabilized laser systems. The determination of precise molecular line parameters has remained limited to accurate line position measurements²² in the ν_3 band of methane. In this article, we report a new approach to real-time mid-infrared Doppler-limited dual-comb spectroscopy. We implement such an approach in the region between 85 and 95 THz (between 3150 and 3500 nm), an atmospheric window that is important for the detection of hydrocarbons as well as oxygen- or nitrogen-containing organic compounds. Precise line parameters, including positions and intensities, are retrieved from spectra measured on the millisecond time scale.

MATERIALS AND METHODS

We describe a setup dedicated to mid-infrared dual-comb spectroscopy. Laser frequency comb oscillators are not readily available in the 85–95-THz region, and dual-comb systems based on nonlinear frequency conversion of mode-locked lasers may be complex and of limited agility. Therefore, we take a different approach, which involves

¹Max-Planck-Institut für Quantenoptik, 85748 Garching, Germany; ²Fakultät für Physik, Ludwig-Maximilians-Universität München, 80799 München, Germany; ³Laboratoire Interdisciplinaire Carnot de Bourgogne, UMR 6303 CNRS – Univ. Bourgogne Franche-Comté, F-21078 Dijon, France and ⁴Institut des Sciences Moléculaires d'Orsay (ISMO), CNRS, Univ. Paris-Sud, Université Paris-Saclay, F-91405 Orsay, France
Correspondence: N Picqué, Email: nathalie.picque@mpq.mpg.de

Received 13 February 2017; revised 28 April 2017; accepted 30 April 2017; accepted article preview online 3 May 2017

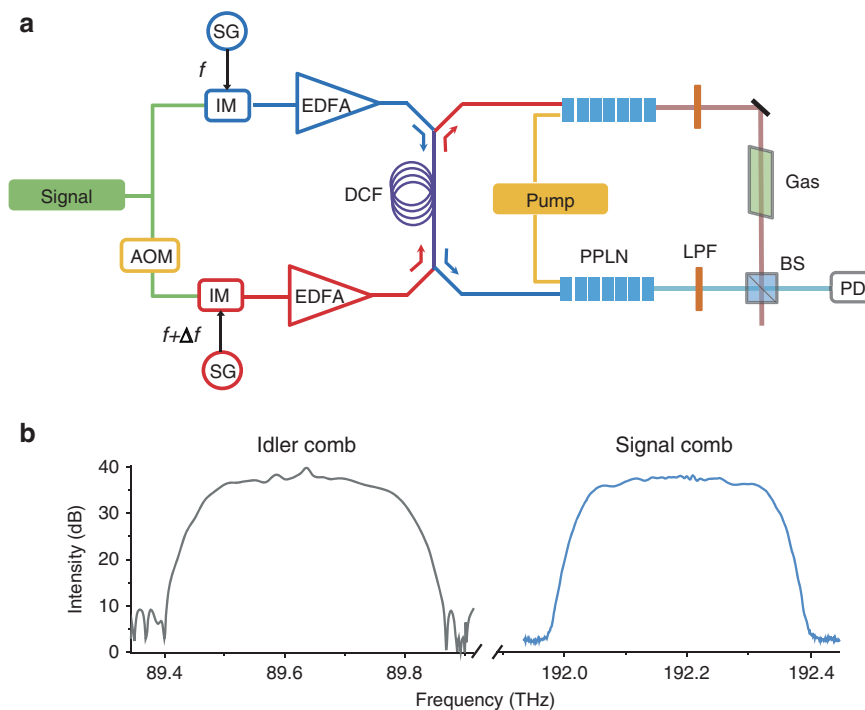


Figure 1 Mid-infrared flat-topped frequency comb generation. **(a)** Experimental setup. AOM, acousto-optic frequency shifter; BS, pellicle beam splitter; DCF, dispersion compensating fiber; EDFA, erbium-doped fiber amplifier; IM, intensity modulator; LPF, long-wavelength-pass filter; PD, photodetector; PPLN, magnesium-doped periodically poled lithium niobate crystal; SG, radio-frequency signal generator. **(b)** Optical spectra of the idler (gray) and signal (blue) combs measured with a Fourier transform spectrometer (Vertex 70, Bruker) at a resolution of 6 GHz. Here, $f_{\text{signal}} = 192.2$ THz (1560 nm), and $f_{\text{idler}} = 89.64$ THz (3344 nm). The resolution of the spectrometer is not high enough to resolve the individual comb lines, which have a line spacing of 300 MHz.

difference-frequency generation of frequency combs based on electro-optic modulators. The experimental setup is illustrated in Figure 1a. We first generate two near-infrared frequency-agile frequency combs in the telecommunication region with a fibered set-up, as already described in Ref. 25. A continuous-wave laser diode (CTL 1550, Toptica, Gräfelfing, Germany), with an optical frequency f_{signal} that is tunable from 185 to 196 THz (1530–1620 nm) at a tuning speed of 1.2 THz s^{-1} (10 nm s^{-1}), is used. The laser diode is pre-calibrated, and its frequency may be chosen via software to a precision within 150 MHz. Finer tuning is not desired for our experiment, although it may be achieved using a piezo-actuator in the external cavity of the diode. The output of the laser diode is split into two arms. In one arm, we shift the frequency of the continuous-wave laser to $f_{\text{signal}} + f_{\text{shift}}$ using an acousto-optic frequency shifter driven at the radio-frequency $f_{\text{shift}} = 25$ MHz. An electro-optic modulator modulates the intensity of each beam. In one arm, the intensity is modulated at a repetition frequency of f and, in the other arm, it is modulated at $f + \Delta f$. The repetition frequencies f and $f + \Delta f$ are chosen to be in the range of 100–500 MHz, and they are set by radio-frequency synthesizers. A straightforward change of electronic filters would shift this frequency range to lower or higher repetition frequencies. After amplification in erbium-doped fiber amplifiers, two asynchronous trains of pulses with an average power of 200 mW and a pulse duration of 50 ps are produced. For spectral broadening, the two pulse trains counter-propagate in a 1.3-km long dispersion-compensating nonlinear fiber. The fiber has a high and flat normal dispersion ($D = -94 \text{ ps nm}^{-1} \text{ km}^{-1}$ at 191.1 THz–1569 nm) and a nonlinear coefficient of $3 \text{ W}^{-1} \text{ km}^{-1}$. When the line spacing f is 300 MHz, the two near-infrared frequency combs comprise $2N + 1 = 1201$ lines each and span 360 GHz (Figure 1b). For a constant average power, the

number of comb lines increases when the repetition frequency decreases. For the first comb, the frequency of each comb line may be written as $f_{\text{signal}} + nf$ and for the second comb, as $f_{\text{signal}} + f_{\text{shift}} + n(f + \Delta f)$, where n is an integer that varies between $-N$ and $+N$. From their beat notes with a tunable laser, the optical comb lines are measured to have a line-width of 3 kHz, which is limited by the resolution bandwidth of the radio-frequency spectrum analyzer. When $N < 1500$, we do not observe any broadening of the lines with increasing n . More details regarding the near-infrared frequency comb generation may be found in Ref. 25.

Each near-infrared signal comb is converted to the mid-infrared by difference-frequency generation between the signal comb and a continuous-wave ytterbium-doped fiber pump laser system (YLR-15k-1064-LP-SF, IPG Photonics, Oxford, MA, USA) of frequency $f_{\text{pump}} = 281.81$ THz (1063.8 nm) in a temperature-controlled 40-mm long MgO-doped periodically poled lithium niobate (PPLN) crystal (MOPO1-0.5-40, Covision, Romsey, UK). Both signal and pump beams are linearly *s*-polarized. At the crystals, the pulse duration of the signal combs is on the order of 300 ps. After the crystals, optical long-wavelength-pass filters (Edmund Optics, York, UK; cutoff at 125 THz–2.4 μm) filter out the light of the pump and of the signal. Two mid-infrared combs are generated (Figure 1b): their center frequencies of f_{idler} and $f_{\text{idler}} + f_{\text{shift}}$ are tunable between 85 and 95 THz (between 3150 and 3500 nm), where $f_{\text{idler}} = f_{\text{pump}} - f_{\text{signal}}$. The line spacings of f and $f + \Delta f$ are the same as those of the near-infrared combs, which are chosen to be between 100 and 500 MHz. The values of the line spacings depend only on electronic settings. The combs have a remarkably flat-topped spectral profile. When the line spacing f is 300 MHz, the idler comb spectrum spans 0.36 THz (13.4 nm), and it includes 1200 lines within 10-dB power variation. The average power

of each idler comb exceeds 500 μW when the power of the pump is 3 W and that of the signal is 150 mW. The conversion efficiency of the PPLN crystals is $\sim 0.28 \text{ mW W}^{-2} \text{ cm}^{-1}$, which is consistent with the specifications provided by the manufacturer. The power per idler comb line is $\sim 420 \text{ nW}$.

A dual-comb interferometer is then realized. One mid-infrared comb is transmitted through a 70-cm long gas cell with CaF_2 windows at the Brewster angle. The comb is combined with the second mid-infrared comb, which acts as a local oscillator, at a 50:50 pellicle beam splitter. To avoid detector nonlinearities, the beam is attenuated to $< 100 \mu\text{W}$ per comb before it is focused onto a fast photodetector (PVI-4TE-5, Vigo System SA, York, UK) of 50-MHz bandwidth. The time-domain interference between the two combs, that is, the interferogram, is digitized by an acquisition card (ATS9462, Alazar-Tech, Pointe-Claire, QC, Canada) at a rate of 180×10^6 samples per second. During the measurement of an interferogram, the frequency f_{signal} of the near-infrared continuous-wave laser is kept unchanged. From one interferogram to another, it can be quickly tuned because of the frequency agility of the extended-cavity laser diode. The acquisition and computation of the interferograms are performed without phase corrections. In addition, no active stabilization is used, which significantly reduces the experimental complexity. The Fourier transform of the interferogram reveals a radio-frequency comb (of a center frequency of f_{shift} and a line spacing of Δf) with the imprint of the mid-infrared molecular absorption lines.

The conversion of the radio-frequency scale to the optical frequency scale in the spectra is performed *a posteriori*. To calibrate the optical frequency scale, the optical frequencies f_{pump} and f_{signal} of the pump and signal near-infrared continuous-wave lasers, respectively, must be measured, as must those of the radio-frequency line spacings f and $f + \Delta f$. All the signal generators, frequency counters, and data acquisition boards used in the experiment are synchronized to the 10-MHz reference signal of an active hydrogen maser (Kvarz CH1-75A, Nizhny Novgorod, Russia). For coarse adjustment, we can monitor these optical frequencies with a wavelength meter (WA-1000, Burleigh, Victor, NY, USA) that has an accuracy of 100 MHz. Such operation is largely redundant given the internal calibration of the frequency f_{signal} of the laser diode, which is precise to within $< 150 \text{ MHz}$, and the day-

to-day stability of the non-tunable frequency f_{pump} of the pump. For precise calibration, the frequencies of the two continuous-wave lasers are referenced to the hydrogen maser via a self-referenced erbium-doped fiber frequency comb. The two continuous-wave lasers are free running. For both lasers, no significant drift is observed on a time-scale of 1 s. The standard deviation of the frequency instabilities of each, measured against the metrological frequency comb, is $< 0.5 \text{ MHz}$ at 1 s. Fizeau-type wavemeters with an accuracy of 10 MHz are commercially available and would represent a simpler calibration alternative, suitable for most of our experiments.

The spectroscopy instrument described above was conceived to overcome the main difficulties of mid-infrared dual-comb spectroscopy. First, dual-comb spectroscopy requires that the coherence between the two combs be maintained during the time of the measurement of the interferogram; otherwise, artifacts severely distort the spectrum. In the near-infrared region, a variety of sophisticated solutions have been successfully employed with mode-locked lasers. They include stabilizing the combs against Hz-line-width continuous-wave lasers⁷ or correcting for the relative drifts of the two lasers, either with analog electronics²⁶ or with digital processing²⁷. Their implementation in the mid-infrared region is more involved.

Here we avoid such complexity by relying on excellent passive relative coherence and common-noise rejection. The two near-infrared combs²⁵ are generated from a single continuous-wave laser and are broadened in the same nonlinear fiber, where they counter-propagate. The pump laser in the difference frequency generation process is common to the two combs. Second, the two mid-infrared combs have a flat intensity distribution. This overcomes the difficulty of the poor dynamic range of mid-infrared photodetectors and fast digitizers. Here, each radio-frequency comb line is measured at a high signal-to-noise ratio, even for short recording times. Third, the moderate spectral span is also favorable to high sensitivity at short measurement times as well as high refresh rates Δf of the interferograms: in dual-comb spectroscopy; both the signal-to-noise ratio and the refresh rate scale with the inverse of the number of spectral elements. To enable signal-to-noise ratio improvements by reducing the spectral span in the dual-comb spectra, the output of mode-locked lasers is often spectrally filtered^{17,22}. Our technique, which inherently

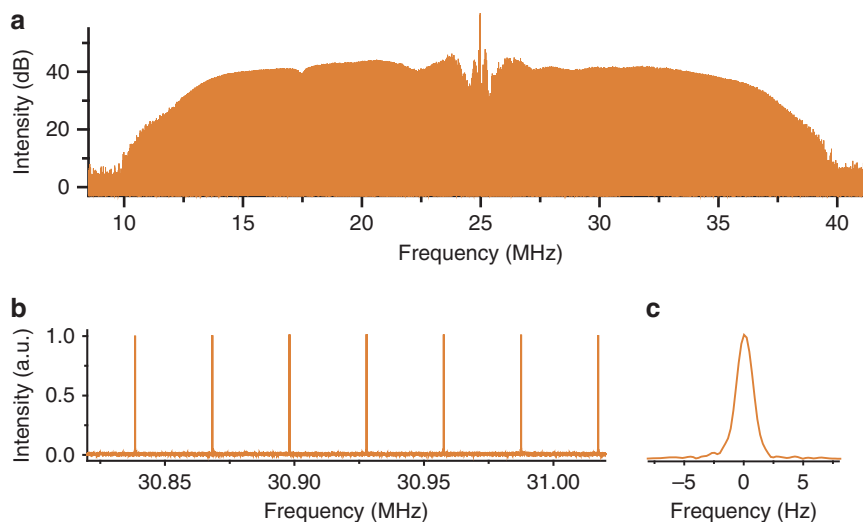


Figure 2 Experimental dual-comb spectrum with resolved comb lines. (a) Radio-frequency spectrum of the detector signal on a logarithmic y-scale. The optical comb line spacing is $f = 230 \text{ MHz}$, and the difference in line spacing is $\Delta f = 0.03 \text{ MHz}$. The spectrum results from a Fourier transform of 198×10^6 samples. (b) Magnified view of a few comb lines on a linear y-scale. (c) In the radio-frequency spectrum, the comb line width is 0.9 Hz, which is limited by the recording time of 1.1 s.

combines moderate spans and fast and mode-hop-free tunability of the spectral position, is a simple alternative to spectral filtering.

RESULTS AND DISCUSSION

We illustrate the excellent passive mutual coherence and the good signal-to-noise ratio in flat-topped dual-comb spectra by performing recordings up to a time-scale of 1 s without any servo-control electronics, adaptive sampling, or phase-correction. Figure 2 shows the radio-frequency dual-comb spectrum of the mid-infrared idlers resulting from a time-domain measurement of 1.1 s duration. The center optical frequency is 89.65 THz, which is mapped in the radio-frequency range at $f_{\text{shift}} = 25$ MHz. The line spacing in the optical domain is $f = 230$ MHz, and in the radio-frequency domain is $\Delta f = 0.03$ MHz. More than 1050 comb lines, spanning 0.25 THz, are resolved with a transform-limited line-width of 0.9 Hz. The signal-to-noise ratio of one comb line is calculated as the maximum of the comb line divided by the standard deviation of the noise floor between two individual neighboring comb lines. The average signal-to-noise ratio for the comb lines across the full-width at half-maximum of the spectral envelope exceeds 1080. We exclude the residual from the continuous-wave carrier from the signal-to-noise ratio determination. Our data acquisition system is limited to a maximum sampling duration of 1.1 s. Within this time limit, the signal-to-noise ratio scales with the square root of the measurement time. In Figure 2, the signal at the frequency $f_{\text{shift}} = 25$ MHz is the residual of the carrier continuous-wave laser. Around f_{shift} , the spectral envelope shows some modulations. Such intensity fluctuations are already present in the spectrum of each near-infrared signal comb, as shown in Ref. 25. These fluctuations are induced by the interaction in the highly dispersive optical fiber between the pulse with a duration of 50 ps at the input of the fiber and the weak residual of the light of the continuous-wave laser. Because electro-optic intensity modulators have a finite extinction ratio (here, 30 dB), a small fraction of the light of the continuous-wave laser is permanently transmitted through the modulator. Such a feeble background is enough to generate a high-contrast dispersive shock wave²⁸. In the frequency domain, an oscillation appears in the spectral shape of the supercontinuum, around the center frequency. The use of electro-optic modulators with a higher extinction ratio would diminish such effect. Around

17.49 MHz (89.61 THz in the optical domain), one can distinguish the nitrogen-broadened $P(3)$ blended manifold of the ν_3 band of $^{12}\text{CH}_4$. The pressure of CH_4 is 13.5 Pa, and the pressure of N_2 is 96×10^3 Pa.

Our short recording times, below 100 μs , are exemplified with a spectrum (Figure 3) of the $P(4)$ manifold of the ν_3 band of methane around 89.3 THz. The dual-comb spectrum is recorded within 76.6 μs at a resolution of 140 MHz. The signal-to-noise ratio culminates at 200, and the spectral span is filtered to 65 GHz for signal-to-noise ratio improvement. The span is moderate but broad enough to simultaneously interrogate several transitions and/or species with a properly centered spectral position. In a measurement time of about 75 μs , the sweep of the frequency of a tunable continuous-wave laser over such a span would be challenging. Here, 465 spectral elements are measured in a multiplex manner at a refresh rate of the spectral acquisition of 13 kHz; this capability provides some interesting opportunities for time-resolved high-resolution spectroscopy of non-repetitive events in the molecular fingerprint region.

Another significant advantage of our frequency comb generators without resonant elements is their freely adjustable line spacing. Their spacing may be selected to match the desired spectral resolution while the measurement times and the refresh rates of the interferograms are kept optimal. In the 3- μm region, for highly crowded spectral features at low pressure, for example, Q branches composed of Doppler-broadened lines, a line spacing f of 100 MHz is desirable. We illustrate our high resolution of 100 MHz with a spectrum in the region of the Q branch of the ν_{11} band of ethylene ($^{12}\text{C}_2\text{H}_4$). The difference in repetition frequencies Δf is set to 15 kHz. The entire spectral span is 230 GHz and includes 2300 resolved comb lines. The recording time of an individual spectrum is 720 μs . The radio-frequency beat notes between the comb lines have a width of 1.39 kHz, which is limited by the measurement time of 720 μs . With a down-conversion factor $\Delta f/f$ equal to 15×10^{-5} , such a width is converted to 9.25 MHz in the optical scale. Such values indicate the good mutual coherence between the combs, as already illustrated in Figure 2. The frequency accuracy of the spectroscopic measurements is determined by the characteristics of the mid-infrared comb that interrogates the sample; we are not equipped to determine optical line-widths in the 3- μm region. The width of the near-infrared comb lines is measured to be narrower than 3 kHz, and the continuous-wave pump laser has a line-width that is

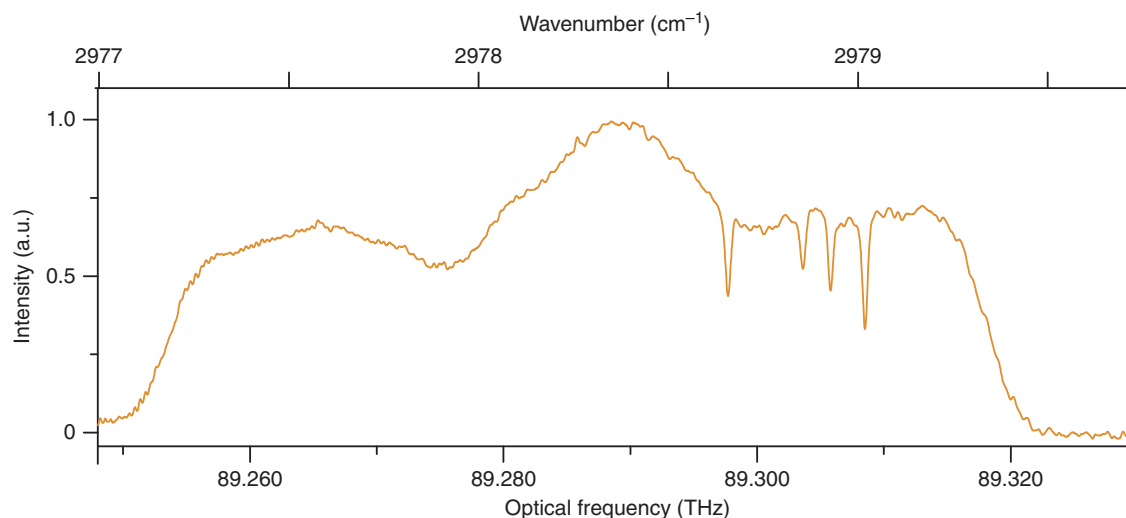


Figure 3 Experimental dual-comb spectrum with a resolution of 140 MHz and a recording time of 76.6 μs . The span is 65 GHz. The transitions belong to the $P(4)$ manifold of the ν_3 band of $^{12}\text{CH}_4$, observed in transmission through a 70-cm long cell filled with 11.4 Pa of methane in natural abundance.

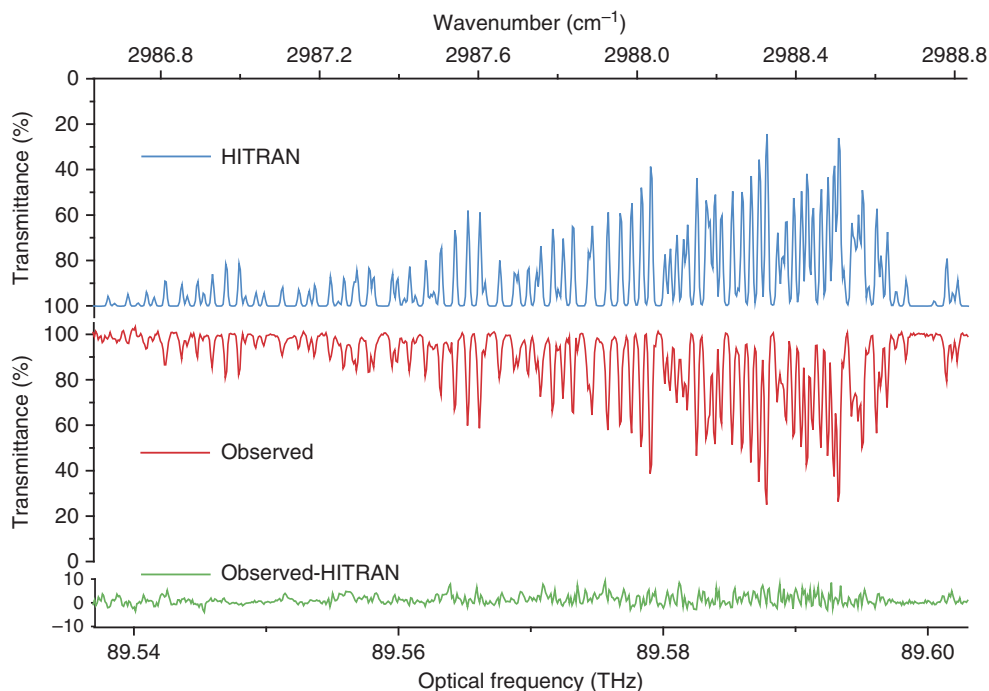


Figure 4 Portion of a dual-comb transmission spectrum showing the crowded Q branch of the ν_{11} band of ethylene. The transmittance signal is plotted at the comb line positions only. The comb line spacing is 100 MHz, and the recording time is 72 ms. The experimental spectrum (red) and a spectrum (mirrored representation, blue) computed from the line parameters available in the HITRAN database²⁹ show good agreement: the 'observed-HITRAN' residuals (green) have a standard deviation of 2%.

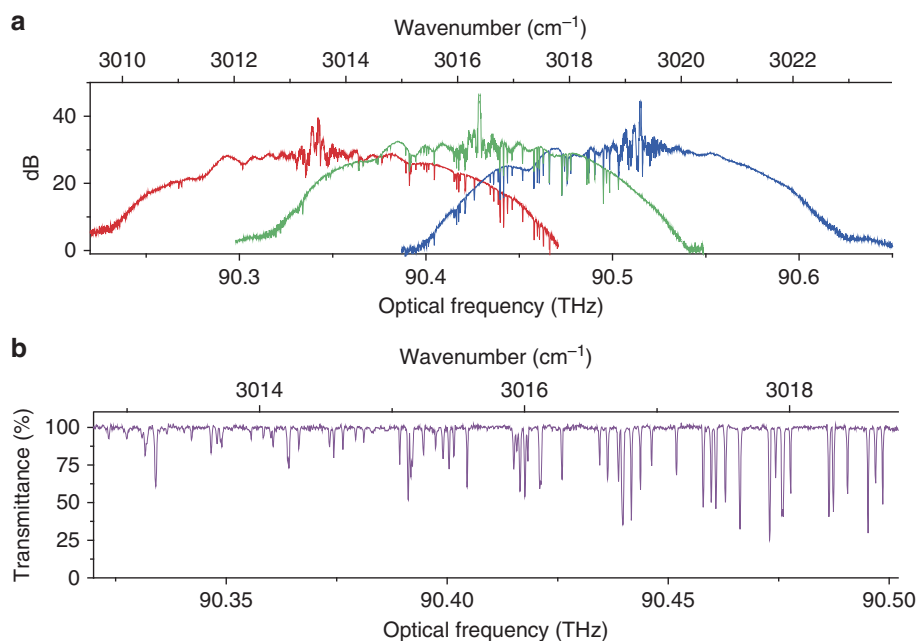


Figure 5 Dual-comb spectra of the Q branch of the ν_3 band of $^{12}\text{CH}_4$ at a resolution of 115 MHz. (a) Three experimental spectra with central frequencies of 90.34, 90.42 and 90.51 THz. (b) Portion of the transmittance spectrum showing the manifolds $Q(2)$ to $Q(12)$.

specified to be narrower than 50 kHz. As discussed below with spectroscopic measurements in methane, the frequency accuracy is currently limited by the instabilities of the free-running continuous-wave pump and signal lasers (0.5 MHz at 1 s for each laser). The spectrum of Figure 4 results from 100 averaged individual spectra for a total measurement time of 72 ms. In Figure 4, a spectral portion of

75 GHz is displayed, where the maxima of the resolved comb lines are plotted. The 70-cm long single-pass cell is filled to a pressure of 140 Pa of ethylene in natural abundance at a temperature of 296 K. The Doppler-broadened full-width at half-maximum of the ro-vibrational lines is 215 MHz; however, in the Q branch, the high density of transitions generates only partly resolved blended lines.

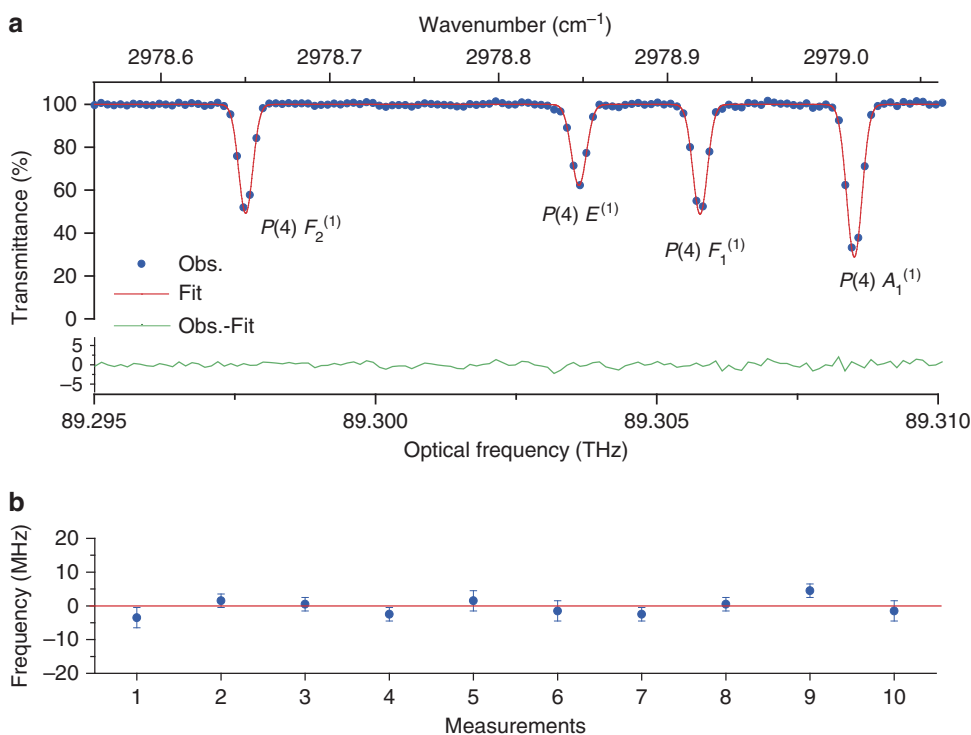


Figure 6 Line parameter measurements. (a) Portion of a dual-comb spectrum showing the $P(4)$ manifold of the ν_3 band of $^{12}\text{CH}_4$. The pressure of CH_4 in natural abundance is 11.4 Pa, and the absorbing path is 70 cm. Gaussian profiles (red) fit the experimental lines (blue dots). The residuals 'Obs.-Fit' (green) do not show any systematic deviation, and their standard deviation is 0.7%. (b) Statistical distribution of 10 measurements of the $P(4)F_1^{(1)}$ line center frequency. The error bar for each measured frequency is the standard error of the fitted line position parameter. The reduced chi-square of the fit is 1.22. The horizontal red line represents the average center frequency (89 305 771.5 MHz), which has been subtracted from each measured frequency for clarity.

Table 1 Center frequencies of the lines in the $P(4)$ manifold of the ν_3 band of $^{12}\text{CH}_4$ measured in this work along with a comparison with the accurate measurements reported in Ref. 32 by Doppler-free saturated absorption spectroscopy and in Ref. 22 by Doppler-limited dual-comb spectroscopy

Assignment	Frequency (MHz)				
	This work	Ref. 32	This work – Ref. 32	Ref. 22	This work – Ref. 22
$P(4) F_2^{(1)}$	89 297 694.9 (12)	89 297 695.2635 (20)	–0.4	89 297 695.06 (30)	–0.2
$P(4) E^{(1)}$	89 303 617.9 (13)	89 303 620.0492 (20)	–2.1	89 303 619.87 (30)	–2.0
$P(4) F_1^{(1)}$	89 305 771.5 (11)	89 305 771.6093 (20)	–0.1	89 305 771.40 (30)	0.1
$P(4) A_1^{(1)}$	89 308 513.3 (11)	89 308 512.2568 (20)	1.0	89 308 512.19 (30)	1.1

Spans broader than 0.3 THz are achieved by tuning the frequency f_{signal} of the signal continuous-wave laser in a step-wise manner and by stitching the resulting dual-comb spectra. Figure 5 illustrates Doppler-limited spectra of $^{12}\text{CH}_4$ in the region of the Q branch of the ν_3 band. The comb line spacing f is 115 MHz and the difference in repetition frequencies is $\Delta f = 20$ kHz. Methane in natural abundance is contained in the 70-cm long gas cell with a pressure of 11.4 Pa at a temperature of 296 K. In Figure 5a, three spectra, each measured within 72 ms at a resolution of 115 MHz, partly overlap. In each spectrum, more than $M = 1800$ comb lines are resolved. The average signal-to-noise ratio for the comb lines across the full-width at half-maximum of the spectral envelope is 350. Therefore, the signal-to-noise ratio per unit of time exceeds $1300 \text{ s}^{-1/2}$, and its product with the number of comb lines is $2.3 \times 10^6 \text{ s}^{-1/2}$. Such a value is higher than that reported in Ref. 22, where combs stabilized against hertz line-width lasers were used. Figure 5b displays a portion of the stitched

spectrum, spanning 185 GHz, with well-resolved Doppler-broadened methane lines and a normalized baseline.

As for any technique of Fourier transform spectroscopy³⁰, dual-comb spectroscopy is prone to subtle artifacts, which can distort the molecular line shapes and provide inaccurate molecular parameters. For assessing our experimental line profiles, we fit a Doppler profile to the tetrahedral sub-level lines $F_2^{(1)}$, $E^{(1)}$, $F_1^{(1)}$ and $A_1^{(1)}$ in the $P(4)$ manifold of the ν_3 band of $^{12}\text{CH}_4$ (Figure 6a). The residuals between the experimental spectrum and its fit have a standard deviation of 0.7%. Importantly, the instrumental line-shape is negligible for the present spectra because narrow comb lines sample the molecular spectrum. The calibration of the frequency scale is performed against the hydrogen maser. The statistical distribution of 10 frequency measurements for the $P(4)F_1^{(1)}$ line position is shown in Figure 6b as an example. The statistical uncertainty corresponds to 0.8 MHz. The frequencies f_{pump} and f_{signal} of the two continuous wave-lasers are

Table 2 Individual intensities of the lines of the $P(4)$ manifold of the ν_3 band of $^{12}\text{CH}_4$ measured in this work

Assignment	Line intensity (cm per molecule)		
	(This work – Ref. 33)/		
	This work	Ref. 33	Ref. 33(%)
$P(4) F_2^{(1)}$	$7.13(13) \times 10^{-20}$	$7.310(147) \times 10^{-20}$	-2.41
$P(4) E^{(1)}$	$4.80(13) \times 10^{-20}$	$4.887(98) \times 10^{-20}$	-1.86
$P(4) F_1^{(1)}$	$7.24(13) \times 10^{-20}$	$7.339(147) \times 10^{-20}$	-1.28
$P(4) A_1^{(1)}$	$1.206(20) \times 10^{-19}$	$1.227(25) \times 10^{-19}$	-1.71

Comparison with the data published in Ref. 33. The temperature is 296 K, and the intensities provided are corrected for isotopic abundance (0.98893 for $^{12}\text{CH}_4$ (Ref. 33)).

each given a conservative uncertainty of 0.5 MHz, which corresponds to their measured instabilities at 1 s. The drifts of the two continuous-wave lasers represent the main source of non-statistical uncertainty. If better accuracies are desired, the two lasers could straightforwardly be actively stabilized. The self-induced pressure shifts in the $P(4)$ manifold have not been reported in the literature to our knowledge. On the basis of measurements in the Q branch³¹, we infer that they are, at 11.4 Pa, significantly smaller than ~ 100 kHz, and we include them in our uncertainty. We neglect the light shift, which has been reported to be (-0.0039 ± 0.0049) kHz μW^{-1} for the $P(7)F_2^{(2)}$ line³². We average the 10 frequency measurements shown in Figure 6b and then measure the center frequency of the $P(4)F_1^{(1)}$ line as 89 305 771.5 (11) MHz. The number within parentheses is the 1σ uncertainty, including statistical and systematic effects, in units of the last digit. Interestingly, we achieve an accuracy that is on the MHz scale for spectra measured within <1 s. We compare our measurements with Doppler-free measurements based on saturated absorption spectroscopy³² (with an accuracy of $\sim \pm 2$ kHz) and Doppler-limited measurements based on accurate dual-comb spectroscopy²² (with an accuracy of ± 300 kHz) and find an agreement that lies within 2 MHz. For line intensity measurements, our estimated overall uncertainty is 4%, primarily caused by the uncertainty on the absolute calibration of the employed capacitance manometer. The line intensities agree within 2.4% with those measured by Pine³³ with an accuracy of 2%. More details on the measured positions and intensities of the lines in the $P(4)$ manifold are given in Table 1 and 2, respectively.

CONCLUSION

Fifteen years ago, combs based on electro-optic modulators had been harnessed³⁴ for a proof-of-principle demonstration of dual-comb optical coherence tomography. In recent years, dual-comb spectroscopy with electro-optic modulators has become a promising approach^{25,35–39} to multiplex spectroscopy. To date, all the demonstrations have been performed^{25,35–39} in the telecommunication near-infrared region. Here we have extended the operation of dual-comb spectroscopy with electro-optic modulators to the mid-infrared range, with first results in the 3- μm region of the CH, OH and NH stretches in molecules. Our technique shows several distinguishing advantages compared to techniques that use systems based on mode-locked lasers. The line spacing and spectral position can be selected quickly and without constraints by simply dialing a knob. Moreover, in contrast to systems with a single electro-optic modulator^{35–37,39} that only generate a limited number of comb lines, our combination of an intensity modulator and a non-linear fiber easily produces a spectrum of more than 1200 lines, which is well suited for simultaneously interrogating several tens of transitions at Doppler-limited resolution within

<100 ms. An optimized design of the nonlinear fiber used for spectral broadening of the near-infrared combs should increase the number of comb lines to beyond 5000. The flat spectral envelope of our mid-infrared combs favors a high signal-to-noise ratio for all comb lines, even at very short measurement times. Our system is designed to generate two combs that are passively mutually coherent. We showed that such design makes it possible to resolve the comb lines of a Fourier-limited width narrower than 1 Hz without active stabilization or phase-lock electronics. Although active stabilization may be required for long averaging times, it would only require easy-to-implement low-bandwidth feedback loops. With further development, the spectrometer can be engineered to be compact and portable. The simplicity of our scheme is particularly meaningful in the mid-infrared region, where high mutual coherence between laser systems that are based on nonlinear frequency conversion, for example, optical parametric oscillators, may be challenging to achieve. Our technique of mid-infrared multiplex spectroscopy over moderate spectral spans offers unprecedented opportunities for rapid measurement of accurate molecular line parameters. For interrogating Doppler-broadened profiles at room temperature, the negligible instrumental line-shape is due to the resolved narrow comb lines. In our set-up, replacing the pump laser of fixed optical frequency with a tunable continuous-wave laser will extend the spectral range of our spectrometer further in the mid-infrared domain. For future applications, for example, trace gas detection, high finesse resonators^{9,39} may enhance the sensitivity to weak absorptions. Differential detection and synchronous detection techniques can also be implemented for noise reduction. Laboratory spectroscopy of transient species and, with further system development, in-field detection of chemical species (for example, pollutants and molecules of atmospheric relevance) may benefit from our novel instrument.

CONFLICT OF INTEREST

The authors declare no conflict of interest.

ACKNOWLEDGEMENTS

European Research Council (Advanced Investigator Grant 267854). Munich Center for Advanced Photonics Max Planck Foundation, IXCORE Fondation pour la Recherche, PARI PHOTCOM Région Bourgogne, Labex ACTION program (Contract No. ANR-11-LABX-0001-01).

- Hänsch TW. Nobel lecture: passion for precision. *Rev Mod Phys* 2006; **78**: 1297–1309.
- Keilmann F, Gohle C, Holzwarth R. Time-domain mid-infrared frequency-comb spectrometer. *Opt Lett* 2004; **29**: 1542–1544.
- Schliesser A, Brehm M, Keilmann F, van der Weide DW. Frequency-comb infrared spectrometer for rapid, remote chemical sensing. *Opt Express* 2005; **13**: 9029–9038.
- Thorpe MJ, Moll KD, Jones RJ, Safdi B, Ye J. Broadband cavity ringdown spectroscopy for sensitive and rapid molecular detection. *Science* 2006; **311**: 1595–1599.
- Coluccelli N, Cassinero M, Redding B, Cao H, Laporta P *et al*. The optical frequency comb fibre spectrometer. *Nat Commun* 2016; **7**: 12995.
- Gohle C, Stein B, Schliesser A, Udem T, Hänsch TW. Frequency comb vernier spectroscopy for broadband, high-resolution, high-sensitivity absorption and dispersion spectra. *Phys Rev Lett* 2007; **99**: 263902.
- Coddington I, Swann WC, Newbury NR. Coherent multiheterodyne spectroscopy using stabilized optical frequency combs. *Phys Rev Lett* 2008; **100**: 013902.
- Mandon J, Guelachvili G, Picqué N. Fourier transform spectroscopy with a laser frequency comb. *Nat Photonics* 2009; **3**: 99–102.
- Bernhardt B, Ozawa A, Jacquet P, Jacquem M, Kobayashi Y *et al*. Cavity-enhanced dual-comb spectroscopy. *Nat Photonics* 2010; **4**: 55–57.
- Schliesser A, Picqué N, Hänsch TW. Mid-infrared frequency combs. *Nat Photonics* 2012; **6**: 440–449.
- Hugi A, Villares G, Blaser S, Liu HC, Faist J. Mid-infrared frequency comb based on a quantum cascade laser. *Nature* 2012; **492**: 229–233.

- 12 Wang CY, Herr T, Del'Haye P, Schliesser A, Holzwarth R *et al*. Mid-infrared optical frequency combs at 2.5 μm based on crystalline microresonators. *Nat Commun* 2013; **4**: 1345.
- 13 Griffith AG, Lau RKW, Cardenas J, Okawachi Y, Mohanty A *et al*. Silicon-chip mid-infrared frequency comb generation. *Nat Commun* 2015; **6**: 6299.
- 14 Kuyken B, Ideguchi T, Holzner S, Yan M, Hänsch TW *et al*. An octave-spanning mid-infrared frequency comb generated in a silicon nanophotonic wire waveguide. *Nat Commun* 2015; **6**: 6310.
- 15 Galli I, Bartalini S, Cancio P, Cappelli F, Giusfredi G *et al*. Mid-infrared frequency comb for broadband high precision and sensitivity molecular spectroscopy. *Opt Lett* 2014; **39**: 5050–5053.
- 16 Villares G, Hugi A, Blaser S, Faist J. Dual-comb spectroscopy based on quantum-cascade-laser frequency combs. *Nat Commun* 2014; **5**: 5192.
- 17 Villares G, Wolf J, Kazakov D, Süess MJ, Hugi A *et al*. On-chip dual-comb based on quantum cascade laser frequency combs. *Appl Phys Lett* 2015; **107**: 251104.
- 18 Bernhardt B, Sorokin E, Jacquet P, Thon R, Becker T *et al*. Mid-infrared dual-comb spectroscopy with 2.4 μm Cr^{2+} : ZnSe femtosecond lasers. *Appl Phys B* 2010; **100**: 3–8.
- 19 Zhang ZW, Gardiner T, Reid DT. Mid-infrared dual-comb spectroscopy with an optical parametric oscillator. *Opt Lett* 2013; **38**: 3148–3150.
- 20 Jin Y, Cristescu SM, Harren FJM, Mandon J. Two-crystal mid-infrared optical parametric oscillator for absorption and dispersion dual-comb spectroscopy. *Opt Lett* 2014; **39**: 3270–3273.
- 21 Smolski VO, Yang HL, Xu J, Vodopyanov KL. Massively parallel dual-comb molecular detection with subharmonic optical parametric oscillators. Preprint at <https://arxiv.org/abs/1608.07318> (2016).
- 22 Baumann E, Giorgetta FR, Swann WC, Zolot AM, Coddington I *et al*. Spectroscopy of the methane ν_3 band with an accurate mid-infrared coherent dual-comb spectrometer. *Phys Rev A* 2011; **84**: 062513.
- 23 Zhu F, Bicer A, Askar R, Bounds J, Kolomenskii AA *et al*. Mid-infrared dual frequency comb spectroscopy based on fiber lasers for the detection of methane in ambient air. *Laser Phys Lett* 2015; **12**: 095701.
- 24 Yu MJ, Okawachi Y, Griffith AG, Picqué N, Lipson M *et al*. Silicon-chip-based mid-infrared dual-comb spectroscopy. Preprint at <https://arxiv.org/abs/1610.01121> (2016).
- 25 Millot G, Pitois S, Yan M, Hovhannisyantsyan T, Bendahmane A *et al*. Frequency-agile dual-comb spectroscopy. *Nat Photonics* 2016; **10**: 27–30.
- 26 Ideguchi T, Poisson A, Guelachvili G, Picqué N, Hänsch TW. Adaptive real-time dual-comb spectroscopy. *Nat Commun* 2014; **5**: 3375.
- 27 Roy J, Deschênes J-D, Potvin S, Genest J. Continuous real-time correction and averaging for frequency comb interferometry. *Opt Express* 2012; **20**: 21932–21939.
- 28 Xu G, Mussot A, Kudlinski A, Trillo S, Copie F *et al*. Shock wave generation triggered by a weak background in optical fibers. *Opt Lett* 2016; **41**: 2656–2659.
- 29 Rothman LS, Gordon IE, Babikov Y, Barbe A, Chris Benner D *et al*. The HITRAN2012 molecular spectroscopic database. *J Quant Spectrosc Radiat Transf* 2013; **130**: 4–50.
- 30 Guelachvili G. Distortions in Fourier spectra and diagnosis. In: Vanasse GA, editor. *Spectrometric Techniques* Vol. II. London: Academic Press; 1982, pp 1–62.
- 31 Pine AS. Self-, N_2 , O_2 , H_2 , Ar, and He broadening in the ν_3 band Q branch of CH_4 . *J Chem Phys* 1992; **97**: 773–785.
- 32 Okubo S, Nakayama H, Iwakuni K, Inaba H, Sasada H. Absolute frequency list of the ν_3 -band transitions of methane at a relative uncertainty level of 10^{-11} . *Opt Express* 2011; **19**: 23878–23888.
- 33 Pine AS. N_2 and Ar broadening and line mixing in the P and R branches of the ν_3 band of CH_4 . *J Quant Spectrosc Radiat Transf* 1997; **57**: 157–176.
- 34 Lee SJ, Widiyatmoko B, Kourogi M, Ohtsu M. Ultrahigh scanning speed optical coherence tomography using optical frequency comb generators. *Jpn J Appl Phys* 2001; **40**: L878–L880.
- 35 Long DA, Fleisher AJ, Douglass KO, Maxwell SE, Bielska K *et al*. Multiheterodyne spectroscopy with optical frequency combs generated from a continuous-wave laser. *Opt Lett* 2014; **39**: 2688–2690.
- 36 Martín-Mateos P, Ruiz-Llata M, Posada-Roman J, Acedo P. Dual-comb architecture for fast spectroscopic measurements and spectral characterization. *IEEE Photonics Technol Lett* 2015; **27**: 1309–1312.
- 37 Martín-Mateos P, Jerez B, Acedo P. Dual electro-optic optical frequency combs for multiheterodyne molecular dispersion spectroscopy. *Opt Express* 2015; **23**: 21149–21158.
- 38 Nishikawa T, Ishizawa A, Yan M, Gotoh H, Hänsch TW *et al*. Broadband dual-comb spectroscopy with cascaded-electro-optic-modulator-based frequency combs. CLEO: Science and Innovations 2015, OSA Technical Digest; 10–15 May 2015; San Jose, CA, USA. Optical Society of America: San Jose, CA, USA, 2015.
- 39 Fleisher AJ, Long DA, Reed ZD, Hodges JT, Plusquellic DF. Coherent cavity-enhanced dual-comb spectroscopy. *Opt Express* 2016; **24**: 10424–10434.



This work is licensed under a Creative Commons Attribution-NonCommercial-NoDerivs 4.0 International License. The images or other third party material in this article are included in the article's Creative Commons license, unless indicated otherwise in the credit line; if the material is not included under the Creative Commons license, users will need to obtain permission from the license holder to reproduce the material. To view a copy of this license, visit <http://creativecommons.org/licenses/by-nc-nd/4.0/>

© The Author(s) 2017